Electrochemical and Solid-State Letters, **9** (3) A156-A159 (2006)
1099-0062/2006/9(3)/A156/4/$15.00 © The Electrochemical Society

Elimination of Extraneous Irreversible Capacity in Mesoporous Tin Phosphate Anode by Amorphous Carbon Coating

Eunjin Kim,[a] Yoojin Kim,[a,b] Min Gyu Kim,[b] and Jaephil Cho[a,*,z]

[a]*Department of Applied Chemistry, Kumoh National Institute of Technology, Gumi, Korea*
[b]*Beamline Research Division, Pohang University of Science and Technology, Pohang, Korea*

Mesoporous tin phosphate with a ~10 nm pore size was synthesized using a sodium-dodecyl-sulfate surfactant as a new anode for a Li-ion cell. The tin phosphate with body centered cubic (bcc) mesostructure exhibited a initial charge capacity of 540 mAh/g, and showed good capacity retention ratio, corresponding to 87% after 20 cycles. Relatively large irreversible capacity (571 mAh/g) ratio of 51%, which impedes the practical application in Li-ion cell, is reduced by the amorphous carbon coating. The coating leads not only to reduced extraneous irreversible capacity ratio of 26% but also improved capacity retention by 11% without changing the first charge cpacity, compared with the uncoated sample. However, intrinsic irreversible capacity loss from the decomposition reaction to tin metal and lithium phosphate phase is unavoidable.
 [DOI: 10.1149/1.2164587]

Manuscript submitted July 13, 2005; revised manuscript received November 22, 2005. Available electronically January 18, 2006.

Mesoporous materials have attracted considerable attention due to their potential applications, such as catalysts and absorbents. They provide excellent opportunities for the creation of materials with additional functionality. Surfactants have been shown to organize a variety of mesopore forms via interactions with ionic species.[1-11] However, except for $AlPO_4$, other phosphates have not received a great deal of attention due to difficulties in forming mesopores.[12,13] Recently, Serre et al.[9] and Mal et al.[10] reported hexagonal and cubic ($Pm\bar{3}n$) mesoporous tin phosphates with pore sizes less than 4 nm using cetyl-trimethyl-ammonium bromide (CTAB) or tetradecyl-trimethyl-ammonium bromide (TTAB). Also, Tian et al.[11] studied tin phosphate with a pore size of ~5 nm, using triblock copolymer (P123). Although tin phosphate is a promising anode material for Li-secondary battery, a larger volume change from tin aggregation during lithium alloying/dealloying leads to a dramatic decrease in the Li storage ability.[14] Recently Kim et al. reported that mesoporous/crystalline tin phosphate composite exhibited reversible pore changes during the Li reaction.[15] They suggested that tin phosphate was first decomposed to an active $Li_{4.4}Sn$ alloy and an inactive amorphous lithium phosphate phase. In addition, the Li_xSn alloy phase can be reversibly dealloyed/alloyed with Li while the lithium phosphate phase serves only as a supporting matrix. On the other hand, pure mesoporous tin phosphates showed significantly larger irreversible capacity with over 60% due to large Brunauer-Emmett-Teller (BET) surface area, corresponding to over 120 m^2/g.[16]

Xiao et al. have proposed the decomposition reaction of the crystalline and amorphous $Sn_2P_2O_7$ phase as follows[14]

$$12.8Li + Sn_2P_2O_7 \rightarrow 2Li_{4.4}Sn + Li_3PO_4 + LiPO_3 \rightleftarrows 8.8Li + 2Sn + Li_3PO_4 + LiPO_3$$

Similarly, amorphous $SnO(B_2O_3)_x(P_2O_5)_y$ proposed Sn metal reduction and the formation of the amorphous matrix phases consisting of B–P–O–Li composites.[17,18] Typically, irreversible capacity loss was approximately between 550 and 660 mAh/g. It was also reported that inherent irreversible capacity linked to the breakdown of the phosphate phases and tin metal, was estimated to ~200–260 mAh/g during the first reduction process, and the remaining extranous irreversible capcity values (~350–400 mAh/g) were reported to be from side reactions with the electrolytes.[14,18,19]

In this study, the large extrinsic irreversible capacity problem from the side reactions in the mesoporous tin-phosphate anode was drastically improved by introducing amorphous carbon coating in the tin phosphate with body centered cubic (bcc) mesopores with ~10 nm pore size. Here, an anionic surfactant, sodium-dodecyl sulfate [SDS: $CH_3(CH_2)_{11}OSO_3Na$], was used as a structure-directing agent.

Experimental

The mesoporous tin phosphate was synthesized by mixing 3.1 g of $SnCl_4$ and 11.4 g of Na_2HPO_4, which was followed by dissolving 40 mL distilled-deionized water (DDW). Subsequently, 10.6 g of HF (10 wt %) was added to the resultant solution with vigorous stirring. When a transparent solution was obtained, 2.9 g of sodium dodecyl sulfate (surfactant) was dissolved in 20 mL of DDW, and the resulting solution was added to a mixture solution of $SnCl_4$ and Na_2HPO_4. The mixture was stirred at 40°C for 1 h and then loaded in an autoclave at 90°C for 12 h. After cooling to room temperature, the precipitate was recovered by centrifugation, followed by repeated washing with distilled water, and dried in vacuum at 100°C for 10 h. The as-prepared mesoporous powders were then calcined at 400°C for 3 h, preserving mesoporous tin phosphate. To coat the tin phosphate particles with the amorphous carbon, glucose (0.5 g) was dissolved in distilled and deoxygenated water (30 mL) until a clear solution was observed, and mesoporous tin phosphate particles (1.2 g) were dispersed in the solution. It was reported that the carbon spheres can be prepared from glucose under hydrothermal condition at 190°C.[17] This is higher than the normal glycosidation temperature, which leads to aromation and carbonization. The mixture was then placed in a 100 mL Teflon-sealed autoclave purged with the Ar, and maintained at 180°C for 3 h. At this temperature, the mesoporous sample was coated with amorphous carbon. The reddish brown products were isolated by centrifugation, washed with water/acetone three times, respectively, and the supernatants were discarded. The carbon content in the carbon-coated sample was measured by a CHS element analyzer. Finally, the powder was calcined at 400°C for 2 h in an Ar atmosphere, and a thermographic analysis (TGA) result showed no weight change up to 400°C, indicating that tin phosphate was not reduced to metallic tin and phosphate phases. In addition, mesoporous tin phosphate was reported to be very stable even at 600°C.[9]

For the electrochemical tests of the mesoporous tin phosphate, the slurry was prepared by mixing the mesoporous tin phosphate, Super P carbon black, and polyvinylidene fluoride in a weight ratio of 4:1:1. On the other hand, for the electrochemical tests of the amorphous carbon-coated tin phosphate, a weight ratio of 5:1:1 (active material: Super P carbon black: polyvinylidene fluoride) was used. A CHS element analysis showed that carbon content in the amorphous carbon-coated tin phosphate was 10 wt %. A mixture of ethylene carbonate/diethylene carbonate (EC/DEC = 1/1 vol %) with 1 M $LiPF_6$ salts was used as the electrolyte. The small-angle X-ray scattering (SAXS) patterns were measured by Cu $K\alpha$ radia-

* Electrochemical Society Active Member.
z E-mail: jpcho@kumoh.ac.kr

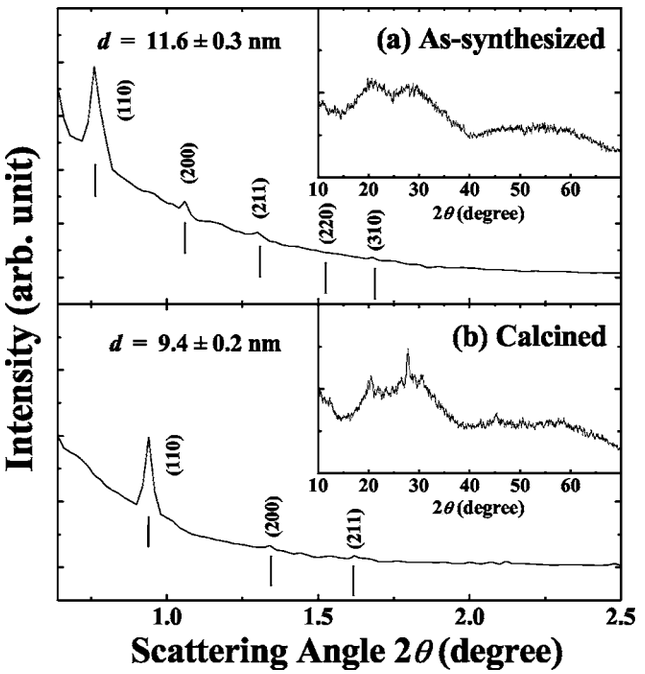

Figure 1. The small-angle X-ray scattering patterns of (a) as-synthesized mesoporous tin phosphate, and (b) mesoporous tin phosphate after annealing at 400°C for 3 h. The corresponding high-angle XRD patterns are shown in the inset.

tion using a Bruker Nanostar. The nitrogen adsorption isotherm was measured at 77 K using a Micromeritics ASAP 2010 analyzer.

Results and Discussion

The SAXS patterns of the as-synthesized and annealed mesoporous tin phosphate are shown in Fig. 1a and b, respectively. Three peaks of the as-synthesized sample are indexed as (110), (200), and (211) [plus weak (310)] confirm a cubic mesoporous structure ($Im\bar{3}m$ space group). (The vertical marks indicate the expected peak positions for bcc.) The corresponding d spacing of the as-prepared mesoporous tin phosphate is 11.6 ± 0.3 nm at the (110) peak ($2\theta = 0.76°$). After annealing (400°C for 3 h), the appearance of the bcc small-angle diffraction peaks indicated that the mesoporous order is preserved, yielding a corresponding d spacing to 9.3 ± 0.2 nm. The high-angle X-ray diffraction (XRD) patterns indicate that some crystal nucleation actually occurred, with the limited formation of nanocrystallite domains.

Figure 2 shows a transmission electron microscopy (TEM) image of the annealed mesoporous tin phosphate with the presence of cubic mesoperiodicity. The corresponding d spacing of the annealed sample, as confirmed by a Fourier transformation, was approximately 10 nm, consistent with the SAXS data. The N_2 adsorption isotherm of the annealed mesoporous tin phosphate is shown in Fig. 3. Barrett-Joyner-Halenda (BJH) analysis shows that the annealed sample exhibits a pore size of approximately 10 nm, which is substantially larger than any of tin phosphates previously reported, and the Brunauer-Emmett-Teller (BET) surface area was ~ 150 m^2/g. To our knowledge, the ordered cubic tin phosphate prepared by SDS has the largest pore size known for an ordered mesoporous tin phosphate.

Figure 4 shows the voltage profiles of the calcined mesoporous tin phosphate. The coin-type half cells containing these were cycled between 1.5 and 0 V at the rate of 65 mA/g (with a Li counter electrode). The mesoporous tin phosphate showed an initial charge capacity of 540 mAh/g and a little capacity decrease to 467 mAh/g after 20 cycles. Note that the difference between first discharge and

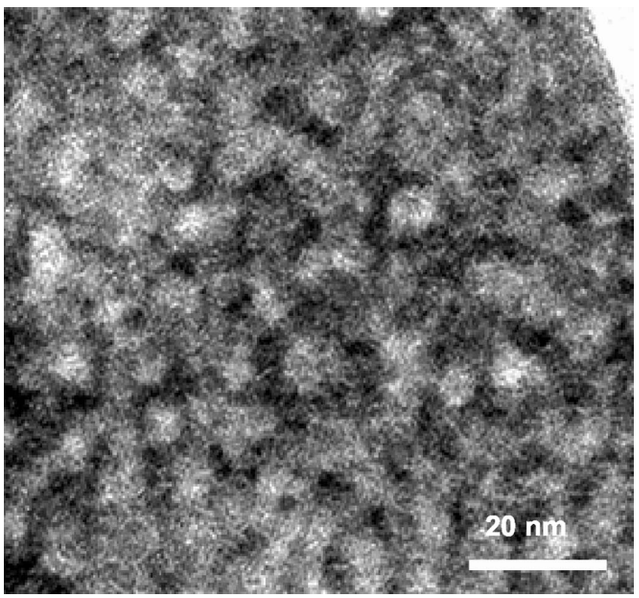

Figure 2. TEM image of the annealed mesoporous tin phosphate.

charge capacities of 1111 and 540 mAh/g, respectively, corresponding to a 51% irreversible capacity ratio. In contrast, amorphous and crystalline tin phosphates showed rapid capacity fading.[18,19] As described in the introduction, the capacity loss from the side reactions between the tin phosphate and the electrolytes need to be eliminated, although an inherent irreversible capacity is unavoidable.

In addition, the cyclability is far superior to the previously reported Sn-based materials that undergo severe capacity fading upon cycling. For example, tin-encapsulated spherical hollow carbon exhibited an initial charge capacity of $\sim$400 mAh/g, which rapidly decreased to 250 mAh/g even after ten cycles.[19] On the other hand, nanoparticle SnO_2 exhibited a rapidly decreasing capacity from its initial value of 700 to 400 mAh/g after only 20 cycles.[20] Both cases did not result in good capacity retention of the Li–Sn alloy. The inset in Fig. 4 shows the small-angle XRD pattern of the mesoporous tin phosphate after 20 cycles. This result indicates that the Li–P–O ma-

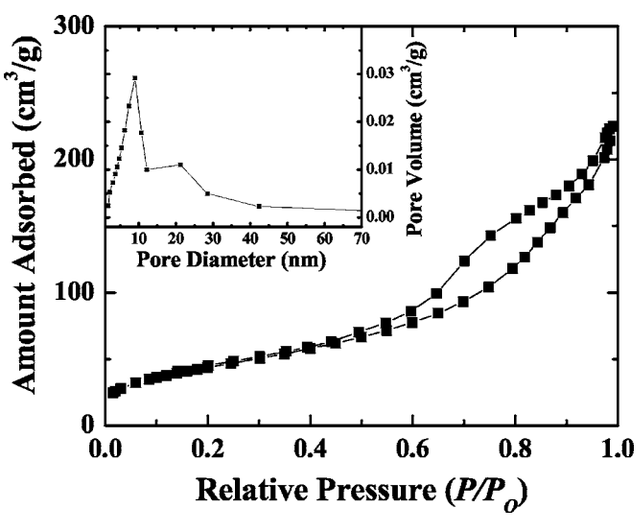

Figure 3. Nitrogen adsorption and desorption isotherms of mesoporous tin phosphate after annealing at 400°C for 3 h. The corresponding BJH distribution is shown in the inset.

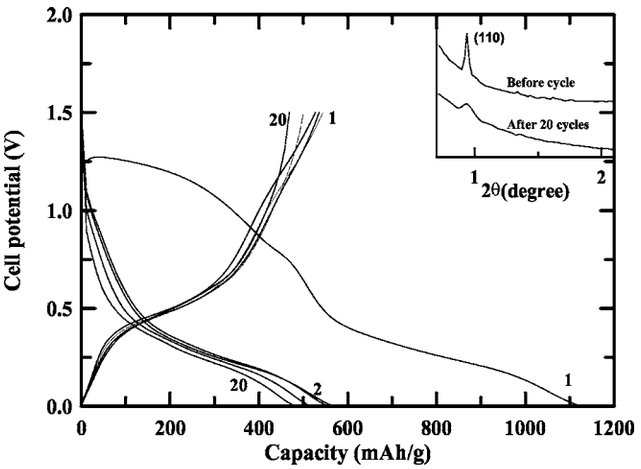

Figure 4. Voltage profiles of the mesoporous tin-phosphate anode, in a coin-type half cell during the 1st, 2nd, 5th, 10th, and 20th cycles between 1.5 and 0V. The inset shows small-angle X-ray peaks before cycling (*d* spacing of 9.3 ± 0.2 nm) and after the 20th cycling (9.3 ± 0.5 nm).

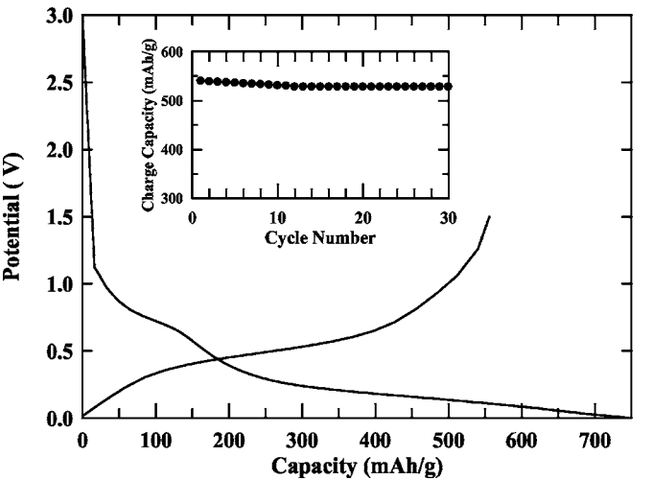

Figure 6. Voltage profile of the amorphous carbon-coated mesoporous tin phosphate between 1.5 and 0 V. The inset is a plot of charge capacity vs cycle number in a coin-type half cell at the rate of 130 mA/g.

trix and Sn particles from the reaction between the tin phosphate and Li are well confined in the pore wall framework. In addition, it clearly shows that the three-dimensional pore frameworks are preserved during cycling. However, the problem of the mesoporous tin material is quite a high irreversible capacity, showing ~51% irreversible capacity as mentioned above. This is related to the high surface area of the tin phosphate, and especially the electrode/electrolyte interface is believed to be a main contributor of the high irreversible capacity. To reduce this, amorphous carbon was directly coated on the tin phosphate. As Fig. 5 shows, rod-shaped tin phosphate particles are covered with amorphous carbon and selective area diffraction (SAD) different pattern showed the presence of the mostly amorphous phase.

Figure 6 shows the voltage profile of the amorphous carbon-coated tin phosphate during the first cycle between 1.5 and 0 V at the rate of 130 mA/g. It exhibited the much reduced irreversible capacity by ~26%, compared with that of the uncoated mesostructured tin phosphate (first discharge and charge capacities of 748 and 550 mAh/g, respectively). That is, the irreversible capacity (561 mAh/g) in the bare sample is reduced to 198 mAh/g after coating. Significant reduction of the extraneous irreversible capacity (363 mAh/g) of the mesoporous tin phosphate after coating is due to the decreased electrolyte reduction on the electrode. The capacity contribution from the amorphous carbon was 12–10 mAh/g since the carbon content in the coated sample was 10 wt % (the first discharge and capacity of the pure amorphous carbon was estimated as 120 and 100 mAh/g, respectively). Considering the mesoporous tin phosphate only, the charge and discharge capacities were estimated to be 538 and 738 mAh/g, respectively. An inherent irreversible capacity (200 mAh/g) that agrees with that reported in crystalline or amorphous tin phosphates[21,22] cannot be reduced by the coating. In addition, capacity retention out to 30 cycles was 97% of the initial charge capacity.

In conclusion, the amorphous carbon coating led to total elimination of the extranous irreversible capacity, although intrinsic irreversible capacity could not be removed. Amorphous carbon-coated mesoporous tin phosphate with bcc structure showed a initial charge capacity of 540 mAh/g with much decreased irreversible capacity by 26%, compared with that of bare mesoporous tin phosphate, and exhibited excellent cyclability (~97% up to 30 cycles).

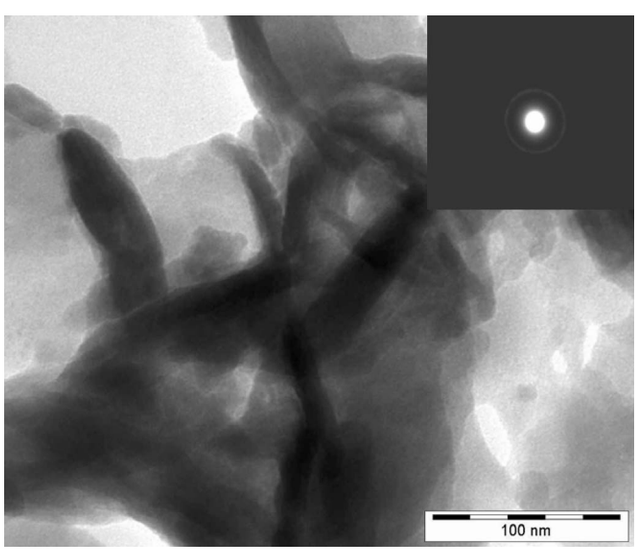

Figure 5. TEM image of the amorphous carbon-coated mesoporous tin phosphate and inset is its SAD pattern.

Acknowledgments

We are grateful to the authorities concerned at Pohang Light Source (PLS) for SAXS measurements. The experiments at PLS were supported in part by Korea MOST and POSTECH. This work was supported by the Ministry of Commerce, Industry and Energy.

Jaephil Cho assisted in meeting the publication costs of this article.

References

1. P. T. Tanev and T. J. Pinnavaia, *Science*, **267**, 865 (1995).
2. A. Vioux, *Chem. Mater.*, **9**, 2292 (1997).
3. N. Ulagappan and C. N. R. Rao, *Chem. Commun. (Cambridge)*, **1996**, 1685.
4. T. Katou, B. Lee, D. Lu, J. N. Kondo, M. Hara, and K. Domen, *Angew. Chem., Int. Ed.*, **42**, 2382 (2003).
5. B. T. Holland, L. Abrams, and A. Stein, *J. Am. Chem. Soc.*, **121**, 4308 (1999).
6. L. Huang, Z. Wang, J. Sun, L. Miao, Q. Li, Y. Yan, and D. Zhao, *J. Am. Chem. Soc.*, **122**, 3530 (2000).
7. P. Yang, D. Zhao, D. I. Margolese, B. F. Chmelka, and G. D. Stucky, *Nature (London)*, **296**, 152 (1998).
8. P. Behrens, *Angew. Chem., Int. Ed. Engl.*, **35**, 515 (1996).
9. C. Serre, A. Auroux, A. Gervasini, M. Hervieu, and G. Ferey, *Angew. Chem., Int. Ed.*, **41**, 1594 (2002).
10. N. K. Mal, S. Ichikawa, and M. Fujiwara, *Chem. Commun. (Cambridge)*, **2002**, 112.
11. B. Tian, X. Liu, B. Tu, C. Yu, J. Fan, L. Wang, S. Xie, G. D. Stucky, and D. Zhao,

Nat. Mater., **2**, 159 (2003).
12. M. Tiemann and M. Fröba, *Chem. Mater.*, **13**, 3211 (2001), and references therein.
13. T. Kimura, Y. Sugahara, and K. Kuroda, *Chem. Commun. (Cambridge)*, **1998**, 559.
14. T. W. Xiao, J. Y. Lee, A. S. Yu, and Z. L. Liu, *J. Electrochem. Soc.*, **146**, 3623 (1999).
15. E. Kim, D. Son, T.-G. Kim, J. Cho, B. Park, K. S. Ryu, and S. H. Chang, *Angew. Chem., Int. Ed.*, **43**, 5987 (2004).
16. E. Kim, M. Kim, and J. Cho, Poster 170, presented at the Quebec, Quebec, Canada, Meeting of the Society, May 15–20, 2005.
17. I. A. Courtney, W. R. McKinnon, and J. R. Dahn, *J. Electrochem. Soc.*, **146**, 59 (1999).
18. I. A. Courtney and J. R. Dahn, *J. Electrochem. Soc.*, **144**, 2843 (1997).
19. M. Behm and J. T. S. Irvine, *Electrochim. Acta*, **47**, 1727 (2002).
20. J. Zhu, Z. Lu, S. T. Aruna, D. Aurbach, and A. Gedanken, *Chem. Mater.*, **12**, 2557 (2000).
21. J. Yang, B. F. Wang, K. Wang, Y. Liu, J. Y. Xie, and Z. S. Wen, *Electrochem. Solid-State Lett.*, **6**, A154 (2000).
22. G. X. Wang, J. Yao, and H. K. Liu, *Electrochem. Solid-State Lett.*, **7**, A250 (2004).